A regional model simulation of the Humboldt system: mean state and propagating variability

Boris Dewitte, IRD/LEGOS, Toulouse, France.

Vincent Echevin, IRD/LODYC, Paris, France.

Oscar Pizarro, PROFC/COPAS, Universidad de Concepcion, Chile.

Abstract

Here, we present the results of a medium resolution, eddy permitting regional model simulation for the eastern south Pacific. Our objective is to investigate the propagating signal in the model and understand how the energy is transmitted both from the open boundaries along the coast and to the inner basin and from the coastal zone to the off-shore ocean.

Comparison with available observations indicates that the model mean state is realistic enough to further investigate the characteristics of the propagating variability along the coast and off-shore. The simulated sea level anomalies are first compared to the TOPEX/POSEIDON satellite derived data. Despite mesoscale variability not well reproduced by the model, the simulated variability has a pattern in rather good agreement with the observations with a comparable decrease of the variability from the coast to the open ocean and southward. A vertical mode decomposition of the simulated pressure field indicates that the sea level variability projects to a large extend on the barotropic and first baroclinic modes. Second and third modes are also energetic, with different patterns along the coast associated with the difference in phase speed of the coastal propagating variability. An extended-EOF analysis of the model baroclinic mode contribution to sea level and zonal current anomalies reveals propagations along the coast and to the west in the form of Rossby waves for the first three baroclinic modes.

Several experiments with and without northern boundary forcing or wind stress variability are carried out in order to delineate the role of coastal Kelvin waves in the triggering process of Rossby waves along the coast. It is show that the instability of the coastal mean current system is not sufficient for explaining the off-shore propagating variability, which characteristics is to a large extend controlled by coastal Kelvin activity.

1 - Introduction

The coastal Peruvian and Chilean region is characterized by permanent upwelling cells in the northern part due to prevailing trade winds and by seasonal upwelling conditions in the southern part. It also exhibits a particular current system called the Peru-Chile Current System (PCCS), extending from central Chile (~40°S) to northern Peru (~4°S). The PCCS is complex, composed of several surface and subsurface currents, and subject to large seasonal and interannual variability. It has received a large interest from the oceanographic and climatic community in recent years for numerous reasons: First, the climate variability off Peru-Chile is highly connected to the tropical Pacific variability, the coast acting as an extension of the equatorial wave guide (Shaffer et al., 1997; Pizarro et al., 2001) and the Cordillera constraining the air flow. The Peru-Chile current is also the most productive among the eastern boundary current (EBC) regions in terms of fish catch (Strub et al., 1998; Carr, 2002), illustrating an intense productivity. Thus the socio-economical impact of climatic events such as ENSO has been large over the region.

In this study we present the results of a medium resolution, eddy permitting regional model simulation. Besides validating some aspects of the model mean state and variability, we investigate the propagating signal in the model and how the energy is transmitted along the coast and from the coastal zone to the ocean interior. The results presented here may be useful for interpreting the data that are being collected, and will provide guidance for further observational studies.

The work is structured as follow. The model, the data and the experiments that were carried out are briefly described in the next section. In section 3, some aspects of the mean circulation and the propagating variability is analysed. Section 4 presents the results of sensitivity experiments to the forcing conditions with the aim to differentiate the roles of local and remote forcings. Section 5 summarizes the results of this study and discusses its relevance to our understanding of the variability in the South eastern Pacific.

2 - Model description and data.

The primitive equation OPA model (Madec et al., 1998) at 1/3° resolution has been set up for the South Eastern Pacific, in the area between 5°S-40°S, 92°W-70°W. This model has 37 z-levels in the vertical with 10m intervals between 0 and 100 m, and 500 m at 4750 m depth. The model has a rigid lid and the sea surface height is calculated diagnostically. The horizontal diffusion on the tracers and velocity is bilaplacian with a constant coefficient of 1.4 10^{11} m^4/s. The model resolution is sufficient to allow some eddies to be resolved explicitly, but the intensity of the mesoscale activity remains relatively low compared to observations (see below).

Open boundary conditions are specified for velocity (barotropic streamfunction and baroclinic velocities), and for the tracers (temperature and salinity) in case of inflow into the model domain. When outflow, tracers are advected out of the domain with an upstream advection scheme. Furthermore, there is a sponge layer to damp propagating waves. The sponge layer is relatively narrow for the north open boundary (1.7°) and wider for the south and west open boundaries (5.3°).

The model is initialised with temperature, salinity and velocity data from the ORCA 2°x2° global model simulation over the same period (Lengaigne et al., 2002). Both models were forced by ERS winds (interpolated first on the 2°x2° ORCA grid, and then re-interpolated over the 1/3° x 1/3° grid, which implies a slight "loss" (change) in small spatial scale variability), NCEP heat fluxes, CMAP precipitation fluxes over 1992-1995.

Several experiments were carried out which settings are summarized in Table 1. 4-year simulations were performed with climatological forcing. 1992 refers to the first year and 1995 to the fourth year.

Name	Period	Boundary forcing	Wind stress forcing	Heat flux forcing
P4 (Control Run)	1992-1995	Monthly climatology	Monthly varying climatology	Monthly varying climatology
P7	1992-1995	Monthly climatology	Annual mean constant	Monthly varying climatology
P8	1992-1995	Mean	Monthly varying climatology	Monthly varying climatology

Table 1: Model experiments' description

3 Mean state and propagating variability.

3.1 Mean circulation and stratification

The annual mean state of the ocean is examined during the fourth year of the climatological simulation, after a statistically steady state has been reached.

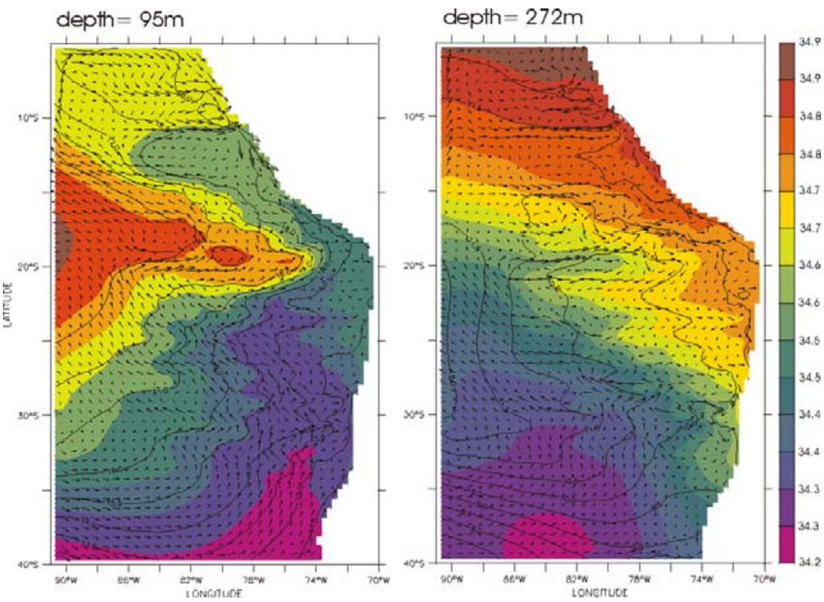

Figure 1: Mean circulation (vectors) and stratification (color for salinity and contour for temperature) at 95m (left) and 272m (right).

The main features of the surface circulation (figure 1a) are consistent with the mean surface height which displays a cyclonic structure centred at 30°S, 90°W near the western open boundary (not shown). Eastward geostrophic surface flow, corresponding to the South Pacific Current (West Wind Drift Current) is present between 30°S and 40°S, and veers to the north near 80°W to become the Chile-Peru Current. Closer to the shore, the surface flow is oriented to the north-west, between 30°S and 20°S. This large scale circulation pattern is modulated by meanders of wavelengths ~300-400 km in the latitude band 30°S-25°S, and in the longitude band between 84°W and the coast. These meanders are due to the baroclinic instability of the large scale Peru-Chile current. Nearer to the coast, the surface flow is oriented northward. It is perturbed by meanders between 25°S and 30°S. East-northeast of the anticyclonic gyre, between 25°S and 18°S, the surface flow is weaker, which is associated a weaker slope of the surface height between 76°W and the coast (not shown). This corresponds to a relatively calm area devoid of strong currents. North of 20°S a large scale circulation pattern is remarkable: the surface flow is oriented north-eastward between 20°S and 15°S, north-westward between 15°S and 12°S and north/north-eastward north of 12°S. To our knowledge, such large scale circulation patterns have not been described in the literature. Poleward surface flow, which would be identified as the Peru-Chile Countercurrent (PCCC) (Strub et al., 1998) can not be clearly identified in the model simulation. This may be due to the lack of resolution of the model, or to a lack of resolution in the wind stress fields. In any case, the dynamical processes responsible for the PCCC remain unclear to the present time (Strub et al., 1998).

At subsurface (figure 1b), the most striking feature is that the model is able to simulate a coastal undercurrent which, although apparently weaker than observed, has a realistic zonal and vertical extent (not shown). Temperature and salinity isolines do not match each other as well as at the surface indicative of different advective processes for salinity and temperature. The poleward extension of the relatively high salinity subsurface waters is rather realistic, whereas the mean upwelling leads to colder surface and subsurface waters near the coast.

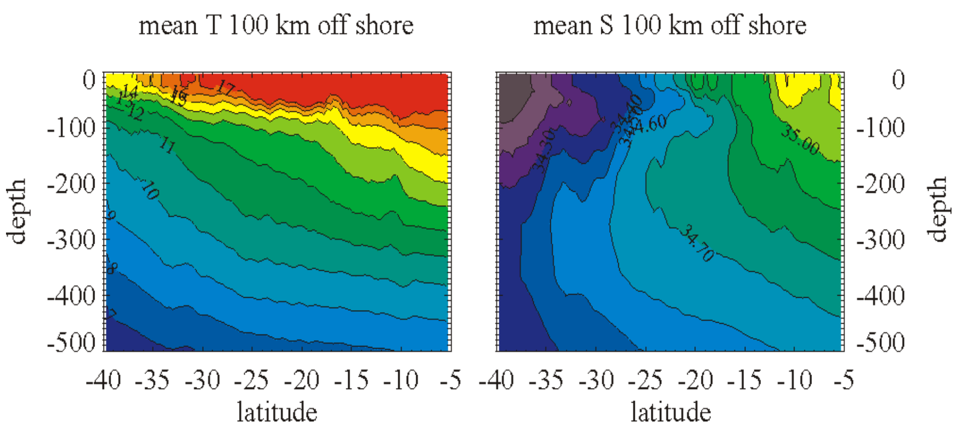

Figure 2: mean (left) temperature (in °C) and (right) salinity (in psu) sections along the coast, 100km offshore, for the first 500 meters.

Mean temperature and salinity alongshore sections at about 100 km offshore is displayed in figure 2 for the 500 upper meters. The isotherms slope upward and southward with a noticeable increase of the slope at 25°S. Similarly, the salinity vertical structure transition zone is at 25°S, with a tongue of low salinity originating from the south around 100-150m (c.f. Schneider et al., 2003). Also apparent is the tongue of relatively high salinity which flows downward towards the south at

~200-300 m, and which corresponds to saline waters of equatorial origin transported by the Peru-Chile Undercurrent (PCU).

The mean stratification along the coast constrains part of the coastal and Rossby wave characteristics. This is investigated in section 3.3.

3.2 surface variability: comparison with satellite data

The simulated sea level variability is compared to the TOPEX/POSEIDON derived sea level data over the 1992-1995 period (figure 3). Note that the data contain the interannual variability contribution due to external forcing although this period is not subject to significant ENSO forcing. The model is able to reproduce the spatial scales of the variability, with in particular the strong mesoscale variability between 25°S and 35°S associated with high eddy kinetic energy (Hormazabal et al., 2004) and the zone of relatively large variability around 15°S-20°S off shore (90°W-80°W). However the model variability is much stronger along the coast which could be partly related to inaccurate altimetric measurements near the coast. The main model flaw is the off shore overall lack in magnitude of the variability which is roughly half the one of the observations. This may be related to the lack of temporal variability in the perpetual, climatological forcing, and to the presence of sponge layers near the open boundaries.

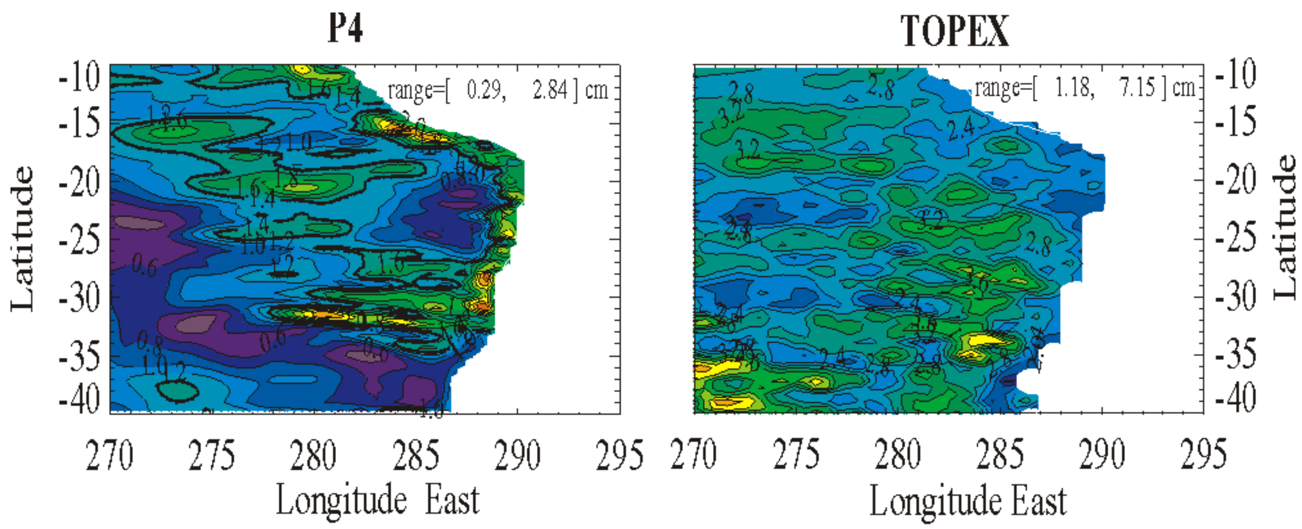

Figure 3: variability map for the control run (P4) and TOPEX/POSEIDON (1992-1995). Units is cm. Contours intervals are every 0.2 cm for P4 and every 0.4 cm for observations.

The result of a vertical mode decomposition of the mean stratification indicates that most of the sea level variability is associated to the barotropic mode and the first three baroclinic modes as shown by figure 4:

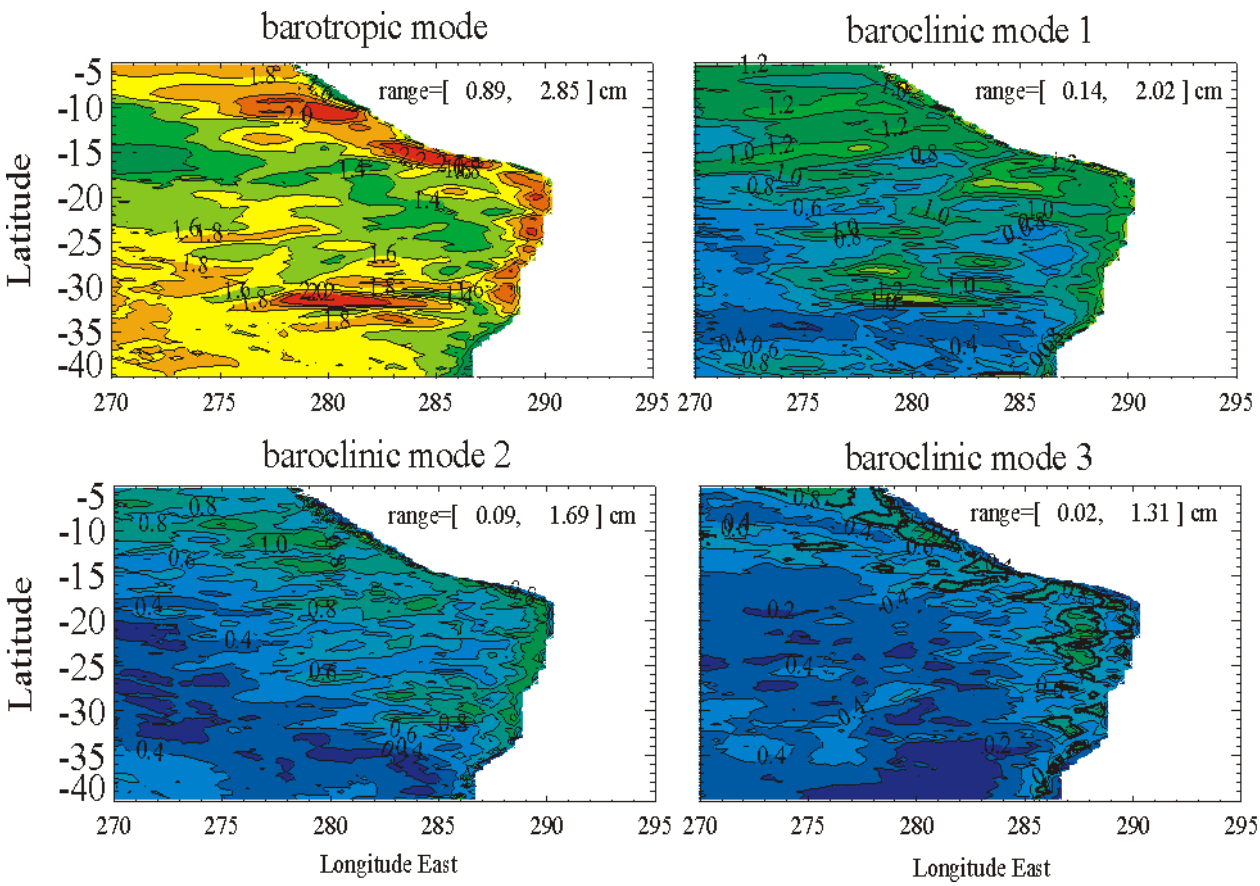

Figure 4: Barotropic and first three baroclinic mode contribution to sea level anomalies for P4. Units are cm. The vertical mode decomposition is done at each grid point of the model grid from the mean simulated stratification, assuming that the mean flow is much lower than the phase speed of the wave (i.e. the effects of the vertical shear on the modal structure and phase speeds can be ignored).

The barotropic mode and the gravest baroclinic mode exhibit a relatively large variability over the whole domain with peaks along the coast and near (32°S; 80°W), whereas the second and third modes are more energetic closer to the coast. As expected from Rossby wave characteristics, the higher the mode order, the closer the maximum variability to the coast. However, it is interesting to note that the variability of the high-order modes does not decrease southward which suggests locally forced variability.

3.3 Propagating variability

along-shore:

Owing to the presence of variability in the open boundary forcing, coastally trapped waves are generated and propagate along the coast. These waves can be especially observed in the intraseasonal band period, in February, June and December for downwelling Kelvin waves, and in April, August for upwelling waves. The propagations occur from 5°S and reach 35°S, at a velocity of ~1.5 m/s, lower than that estimated by Ulloa et al.(2001) for intraseasonal wave packets during the 1997-1998 El Niño. The phase velocity is faster between 10°S and 15°S, and there is a change at 15°S which may be due to bottom topography effect, as suggested by the calculation of the theoretical phase speed from the model stratification (not shown).

cross-shore :

Westward propagation is also observed in the model simulation at intraseasonal and seasonal timescales. Part of the signal originates at the coast and is coherent with the propagating coastal signal, where part of it is apparently forced offshore or/and is triggered by the instability of the mean flow. The vertical mode decomposition of the current variability allow to better identify the propagating characteristics. Interestingly the zonal current variability projects on a few vertical modes (figure 5) with the second and third modes as energetic as the gravest mode on average in the northern region. Southward, the relative contribution of the high-order modes increase due to the change in stratification and forcing.

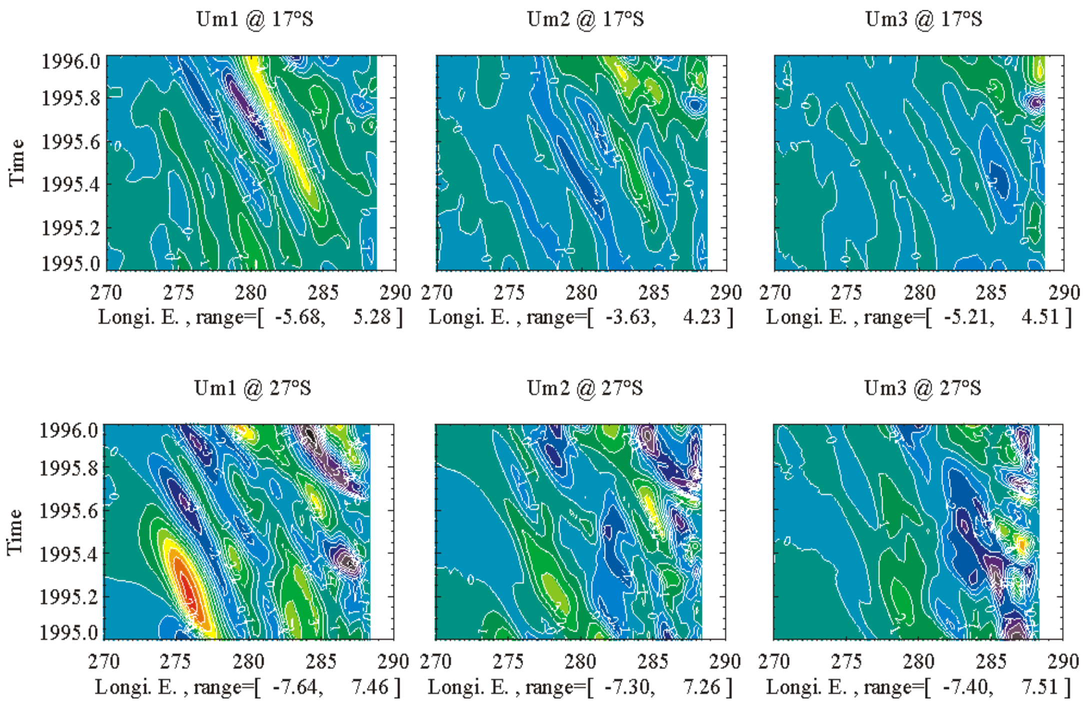

Figure 5: Baroclinic mode contributions to the cross-shore current anomalies in 1995 at (top panel) 17°S and (bottom panel) 27°S for the first three modes of P4. Units is cms^{-1}. Contour interval is every 1 cm s^{-1}.

4. Role of boundary forcings.

Several sensitivity experiments were performed to investigate the source of variability along the coast and off-shore (see Table 1). The results are displayed in Figure 5 for the sea level variability in 1995.

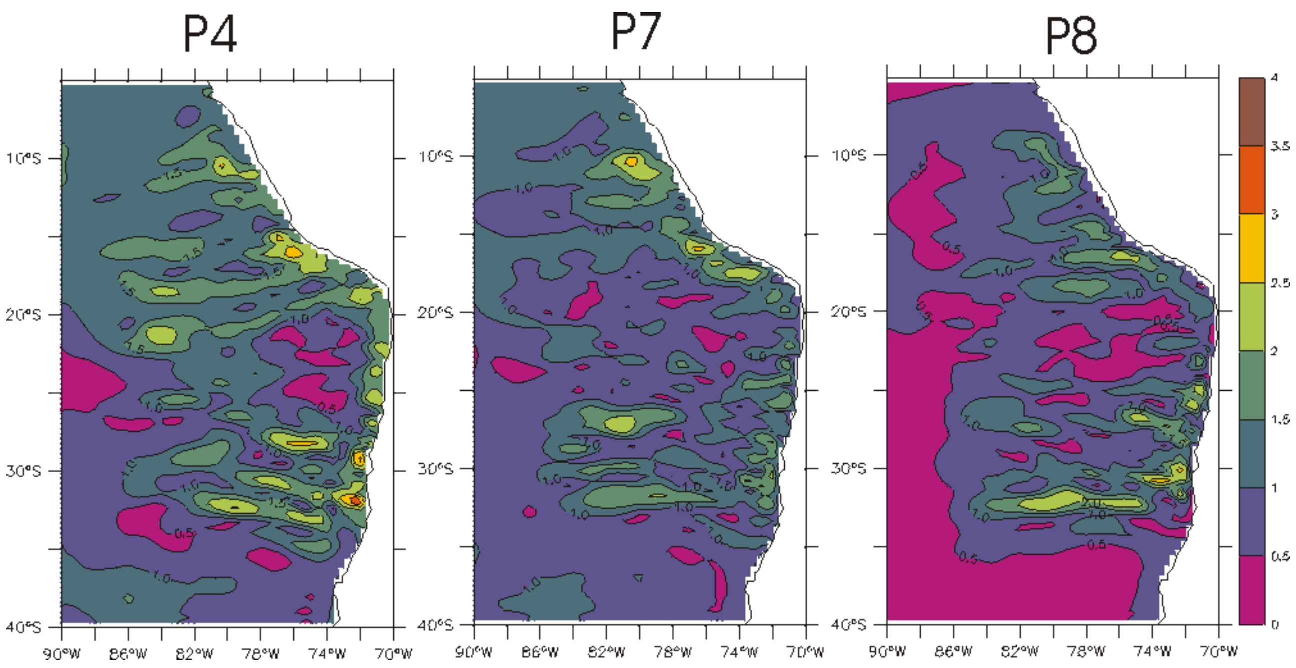

Figure 5: sea level variability (1995) for the 3 experiments, i.e. the control run (P4), the experiment without wind stress forcing variability (P7) and the experiment without variable boundary forcing (P8). Unit is cm.

They indicate that the sea level variability along the coast is mostly controlled by the open boundary forcing at the northern boundary, and related to the propagation of coastal Kelvin waves. The amplitude of the waves in P7 is very similar to that in the control simulation P4. Sea level variability is stronger in the south near 25°S-30°S in P4 and P8 owing to the variability of wind stress curl and alongshore wind stress. In P8 no propagations along the coast were observed leading to a slightly weaker variability of sea level at the coast compared to P4 and P7. However, the sea surface variability, although weaker, is spatially structured very much like that in the control run. In particular, the zone of large variability in the southern region 25°S-35°S seems to be independent of the presence of wind forcing or of Rossby waves generated at the coast. More likely, its seems to be related to the mean position of the South Pacific Current (SPC), which, in our simulation, flows over a ridge near 34°S, 81°W-77°W. This topographic feature is likely to generate instabilities of the SPC in its lee.

The inter-comparison of the cross-shore propagations in these various simulations suggest that the triggering mechanism of the Rossby wave near the coast may be associated to the instability of the mean current system and do not necessarily correspond to the crossing of the coastal Kelvin wave. Local wind stress forcing favors the growing amplitude of the Rossby waves but its impact varies with latitude.

5. Conclusions

A medium resolution regional model simulation of the Peru-Chile Current System was presented. The model exhibits skills in reproducing some aspects of the observed mean state and variability, namely the main currents, the mean stratification and the alongshore and cross-shore propagating variability. The model allows to investigate the characteristics of the sea level and current disturbances that propagate along the study region and the mechanisms involved in their triggering and maintenance as a function of the forcing conditions. Results indicate that Rossby wave variability is related to local wind stress forcing and coastal Kelvin variability through a non-linear function. Rossby wave propagation is indeed either present in the simulation with and without boundary forcing or with and without wind stress curl forcing and their characteristics vary in each case. The vertical mode decomposition of the model stratification also reveals a significant contribution of the high-order modes, which relative contribution increased southward as the thermocline shallows. This, in particular, suggests a different impact of the dynamics on SST changes as a function of latitude. The analysis of such impact could help to interpret the peculiarities of the different upwelling cells present along the Peru-Chile coast. This is currently under investigation. At last, the results presented in this study are encouraging for future progress in seasonal forecasting in this region.

Acknowledgments: The preparation and development of this work were made possible thanks to several stays funded by ECOS (grants N# C03U05) of D. B. Dewitte and O. Pizarro at PROFC and LEGOS.

References:

Blanco J.L., A.C. Thomas, M.-E. Carr, and P.T. Strub, 2001: Seasonal climatology of hydrographic conditions in the upwelling region off northern Chile, J. Geophys. Res., 106,C6, 11,451-11,467.

Carr, M.-E., 2002: Estimation of potential productivity in eastern boundary currents using remote sensing. *Deep Sea Res.*, Part II, **49**, 59-80.

Clarke A. J. and C. Shi, 1991: Critical frequencies at ocean boundaries. *J. Geophys. Res.*, **96**, 10,731-10,738.

Hormazabal S., G. Shaffer, and O. Leth, 2004: The coastal transition zone off Chile. *J. Geophys Res.*,109, C01021, doi:10.1029/2003JC001956.

Lengaigne, M., J.-P. Boulanger, C. Menkes, S. Masson, G. Madec, and P. Delecluse, 2002: Ocean response to the March 1997 Westerly Wind Event. *J. Geophys. Res.*, 107 (C11), 10.1029/2001JC000841.

Leth, O., and G. Schaffer, 2001: A numerical study of seasonal variability in the circulation off central Chile, *J. Geophys. Res.*, **106**, 22,229-22,248.

Madec, G., P. Delecluse, M. Imbard, and C. Lévy, 1998: OPA 8.1 Ocean General Circulation Model reference manual. Note du Pôle de modélisation, Institut Pierre-Simon Laplace, N°11, 91pp.

Pizarro, O., A. J. Clarke and S. V. Gorder, 2001: El Niño sea level and currents along the South American coast : comparison of observations with theory. *J. Phys. Oceanogr*., **31**: 1891-1903.

Pizarro, O., 1999: Low frequency fluctuations in the eastern boundary current off south America: remote and local forcing. PhD thesis, Department of Oceanography, Earth Sciences Center, University of Göteborg.

Schneider W., R. Fuenzalida, E. Rodriguez-Rubio, and J. Garces-Vargas, 2003: Characteristics and formation of Eastern South Pacific Intermediate water. *Geophys. Res. Lett.*, Vol. 30, No. 11, 1581-1584.

Shaffer, G., O. Pizarro, L. Djurfeldt, S. Salinas and J. Rutlland, 1997: Circulation and low-frequency variability near the Chilean coast: remotely forced fluctuations during the 1991-92 El Niño. *J. Phys. Oceanogr.*, **27**: 217-235.

Strub, P. T., J. M. Mesias, V. Montecino, J. Rutllant and S. Salinas, 1998: Coastal ocean circulation off western South America. The Sea, Vol. 11, edited by A. R. Robinson and K. H. Brink, pp. 273-313, John Wiley, New York.

Ulloa, O., R. Escribano, S. Hormazabal, R. A. Quiñones, R. R. González and M. Ramos, 2001: Evolution and biological effects of the 1997-98 El Niño in the upwelling ecosystem off northern Chile. *Geophysical Research Letters*, 28: 1591-1594.